

Research Article

Effects of the Hypoxia-Mimetic Agents DFO and CoCl_2 on HeLa-Fucci Cells

Baptiste Bedessem*, Marie-Paule Montmasson, Malika Hamel, Françoise Giroud and Angélique Stéphanou

UJF-Grenoble 1, CNRS, Laboratory TIMC-IMAG/DyCTiM, UMR 5525, Grenoble, France

Abstract

The Fucci system is a promising model to study the cell cycle *in vivo* and *in vitro*. Because it enables to follow the progression of the cycle using fluorescent microscopy, it can be used to precisely visualize the effects of external strains on proliferation. However, it was reported that the lack of oxygen strongly affects the fluorophores used in the HeLa-Fucci cell line. As a consequence, it limits its use in hypoxic conditions. To study the effects of hypoxia on cell proliferation by using this cell line, one could use HiF-1 α inducers, such as CoCl_2 and DFO, which are often used as hypoxia-mimetic agents. As these iron-chelators also have anti-cancer properties, their biological effects were studied in various experimental conditions. A great variability of actions were reported. In this study, we investigate for the first time their effects on HeLa-Fucci cells proliferation dynamics. We find that CoCl_2 has a biphasic effect on the cell cycle, by promoting or inhibiting the progression into the G1-phase. In presence of DFO, we identified an arrest in the G2-phase, which follows a switch-like behavior. These observations bring original results since iron-chelators are mainly known to induce an arrest at the G1/S transition. They also provide specific information about the possibility to use Fucci cells to study the influence of hypoxia on the cell cycle. Finally, by considering the known genetic characteristics of HeLa cells we propose a hypothesis to explain the particular response of Fucci cells to DFO and CoCl_2 . The discussion proposes a plausible action of DFO and CoCl_2 on the MAPK pathway.

Keywords: CoCl_2 ; DFO; HeLa Fucci-cells; Hypoxia; MAPK

Background

The Fucci (Fluorescent Ubiquitination-Based Cell Cycle Indicator) cell is a recently created line of HeLa cells (cervix carcinoma) [1]. This system uses a couple of oscillating cell cycle proteins, cdt1 and geminin, respectively labeled with monomeric Kusabira Orange 2

*Corresponding author: Baptiste Bedessem, UJF-Grenoble 1, CNRS, Laboratory TIMC-IMAG/DyCTiM, UMR 5525, 38041 Grenoble, France, Tel: +33 0456520045; E-mail: baptiste.bedessem@imag.fr

Citation: Bedessem B, Marie-Paule M, Hamel M, Giroud F, Stéphanou A (2015) Effects of the Hypoxia-Mimetic Agents DFO and CoCl_2 on HeLa-Fucci Cells. J Cell Biol Cell Metab 2: 004.

Received: February 13, 2015; **Accepted:** March 12, 2015; **Published:** March 26, 2015

and monomeric Azami Green. As a consequence, the G1, S, and G2/M phases are labeled with different colors. This cell line is useful to quantify the duration of each phase of the cycle, and to determine the percentage of cycling and non-cycling cells in a non destructive way. Notably, it can be used to visualize *in vivo* the progression of the cycle [2,3]. *In vitro*, it is a good tool to observe the effects on cell dynamics of various environmental strains, such as hypoxia. The study of the cellular and molecular effects of hypoxia is one of the important challenge of modern biology. Indeed, it is well established that tumor cells undergo chronic hypoxia, due to the limit of oxygen diffusion in the cancer tissue [4,5]. This chronic hypoxia correlates with an increased resistance to chemotherapy [6,7]. Notably, hypoxia activates anti-apoptotic pathways [8] and can induce proliferation of cancer cells. Indeed, even though hypoxia is known to induce cell cycle arrest in G1 phase [9], it was shown that chronic hypoxia can also stimulate proliferation in various cell lines [10-13]. In a general way, it seems that a balance exists between death and survival/proliferating pathways, depending on the duration and severity of the hypoxic event [14]. The complexity of the cellular response to hypoxia is controlled by the HiF-1 α factor, which accumulates when oxygen is lacking [15]. This factor activates signaling pathways which regulate proliferation and death. It was often observed that HiF-1 α accumulates in cancer cells [16,17]. This accumulation can be due to the physiological chronic hypoxia of cancer cells or genetically determined, for instance by the mutations affecting the Von Hippel-Lindau (VHL) gene [18].

However, the study of the effects of hypoxia using HeLa-Fucci cell line is complex since the lack of oxygen was shown to modify the fluorescence of Kusabira Orange and Azami Green, as shown by Kaida et al., [19,20]. This artefact makes difficult the use of HeLa-Fucci cells in real hypoxic conditions. As a consequence, the study of the effect of the hypoxia pathway, notably the stabilization of HiF-1 α , on cell cycle dynamics using this cell line could be done through the use of hypoxia-mimetic chemicals. Indeed, various molecules can be used to mimic hypoxia by inducing HiF-1 α accumulation, such as Cobalt Chloride (CoCl_2), Dimethylxalylglycine (DMOG), Desferrioxamine (DFO). These molecules are also studied for their anti-cancer effect, as iron-chelators [21,22]. In a general way, they induce HiF-1 α accumulation, but they also have numerous HiF-1 α -independent effects [23]. Notably, they are known to induce apoptosis [8] and cell cycle arrest through complex interactions with regulating proteins [22]. CoCl_2 and DFO are certainly the most commonly used hypoxia-mimetic molecules [24]. As a consequence, their biological effects were relatively well tested over the last years. They both induce apoptosis when their concentration is high enough [8,25,26]. However, CoCl_2 seems to promote cell survival during the first 6-8 hours of treatment [27,28]. Cell proliferation in presence of these agents was assessed using different cell lines. Dai et al., (2012) [25] have shown that in presence of CoCl_2 , PC-2 cells growth was stimulated during 72h. Then, a dose-dependent inhibition of growth was observed, with an increase of the cell death rate. In a general way, CoCl_2 and DFO are known to inhibit cell proliferation [24]. However, their precise influence on cell cycle is variable. In presence of CoCl_2 , some studies report an arrest in the G1 phase [24,29], or in the G2 phase [30]. In the case of DFO, it is not clear if DFO blocks the cell

cycle in G1, S, or G2 phase. Many studies report an arrest on G1 phase or in S phase, depending on dose and cell type [24,31-33]. A recent paper by Siriwardana et al., [34] could precisely differentiate a mid-G1 phase arrest and a S phase arrest. This result suggests that these two types of cell cycle blockage act more or less in presence of DFO, depending on cell line. In the other hand, some authors also noticed an arrest during the G2 phase [22,35]. Clearly, the effects of DFO and CoCl₂ on cell cycle dynamics closely depend on the dose used, the time of exposure, and the cell line studied.

As a consequence, in order to use these molecules as HiF-1 α inducers or anti-cancer agents on HeLa-Fucci cells, a preliminary study of their biological effects on this cell line is required. Notably, it is crucial to characterize their effect on the cell cycle, using the fluorescent properties of the Fucci cells. It would also bring additional knowledge on the biological response to these anti-cancer molecules. This work thus proposes, for the first time, to investigate the effects of iron-chelators DFO and CoCl₂ on HeLa-Fucci cells proliferation dynamics. We constructed our study as follows. We first verified that a lack of oxygen generates fluorescence extinction, even in moderate hypoxia (3% O₂). To evaluate the toxicity of DFO and CoCl₂, we studied their influence on cell death and cell growth of HeLa-Fucci cells. This first step is necessary to rigorously interpret the fluorescent data. It also provides interesting comparative results of the cellular effects of the two molecules. Then, we studied their actions on the cell cycle dynamics of HeLa-Fucci cells. We show that this cell line exhibits an original response to iron-chelators DFO and CoCl₂, quite different from observations obtained with other cell lines, which have mainly shown an arrest at the G1/S transition [22]. In our experimental conditions, DFO generates a G2 phase arrest of the cell cycle when its concentration passes over a threshold. CoCl₂ acts on cell proliferation following a complex biphasic effect. Depending on dose and time of exposure, it promotes or inhibits the entry into the cycle. By using some known elements of the genetic characteristics of HeLa cells, we propose a molecular mechanism to explain our observations. It gives a hypothesis to test the action of DFO and CoCl₂ on the MAPK pathway.

Methods

Culture conditions

HeLa cells expressing the Fucci probes (HeLa-Fucci) were provided by the RIKEN BRC through the National Bio-Resource Project of MEXT, Japan. Cells were maintained in DMEM (PAA, Piscataway, NJ), with 10,000 U/ml of penicillin-streptomycin and 10% of fetal bovine serum at 37°C in a 5% CO₂ humidified atmosphere. For CoCl₂ and DFO treatments, a 50 mM solution of CoCl₂ and a 20 mM solution of DFO were prepared by dissolving cobalt chloride (Cobalt (II) Chloride hexahydrate, Sigma-Aldrich, Saint-Louis, MO) and DFO (Deferoxamine mesylate, Sigma-Aldrich, Saint-Louis, MO) in ultra-pure water. Defined volumes of these solutions were added to cells previously cultured for 12 hours on one chamber Lab-tek cover-glasses (initial concentration: 1.10⁵ cells per ml). All experiments are compared to control groups. Cells in control groups were cultured in the same conditions than the DFO or CoCl₂ groups, but without any chemicals.

For the experiments in hypoxia we used a SANYO MCO-5M cell culture incubator which allows one to impose various conditions of oxygen pressure on the cells.

Cell death measurements

The number of cells and the level of cell death were determined using Trypan Blue. After treatment with trypsin, 20 μ L of cells in DMEM were mixed with 20 μ L of Trypan Blue (Trypan Blue 0.4%, Invitrogen, Eugene, Oregon). Cell concentration and viability were automatically determined using Invitrogen Countess Automated Cell Counter. The experiments were performed in quadruplicate cultures. Statistical analysis was performed to compare mortality ratio and cell concentration for the different experimental conditions. We applied Student tests to compare average values.

Fluorescent imaging

Fluorescent images were taken using a Z1 Axio Observer inverted fluorescent microscope (ZEISS, Jena, Germany). This microscope is equipped with a EMCCD Camera (Hamamatsu C9100-13) and is piloted with the AxioVision software. For each cover-glass, corresponding to the different experimental conditions, images were taken with three canals (GFP, Texas-Red and Bright Field), in 40-60 fields, representing a total of about 4000 cells after 48h of growth in normoxic conditions and 10000 cells after 96h.

Cell cycle phases definition

The definition of the different cell cycle phases was originally presented by Sakaue-Sawano et al., [1]. It was then notably used by Nagano et al., [36]. Figure 1A presents the classical definition of the cell cycle phases in the Fucci system, and figure 1B presents a microscopic field where all phases are visible and can be distinguished. Cells with a visible red fluorescence are considered to be in the G1 phase, green cells are in the G2 phase, red and green cells are in the S phase. Cells in the M phase are not fluorescent. Since our study specifically considers the entry into the G1 phase, we named G0/G1init the phase of the non-fluorescent cells which are not in the M phase. G0 stands for the quiescent state and G1init stands for the very beginning (i.e., initiation) of the G1 phase. Indeed, biologically, these cells can be in a quiescent state or in the early G1 phase [1]. The M and G0/G1init phases were distinguished using a morphological criterion (Figure 1). This criterion is based on the classical tools used to identify mitosis in cell cultures. This phase is highly recognizable since the cells take a typical morphology, characterized by a spherical shape and the absence of nucleus.

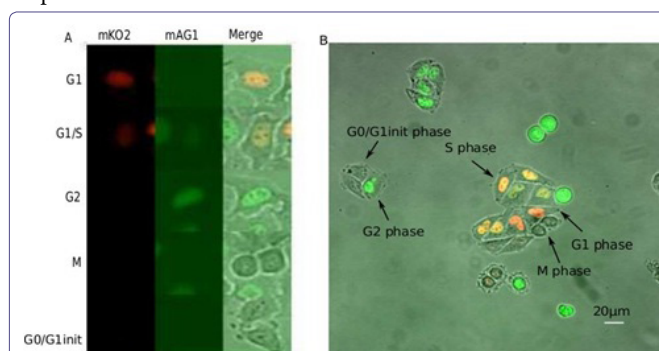


Figure 1: Fluorescent images of HeLa-Fucci cells.

A. Criteria for the classification of Fucci cells into each cell cycle phase. From the left to the right: red channel, green channel, and merge of red, green and bright-field channels. Red cells are in the G1 phase, cells with both red and green fluorescence are in the S phase, green cells are in the G2 phase. Non-fluorescent cells are in M or G0/G1init phase. These two phases are differentiated with morphological criteria;

B. Example of a microscopic field with Fucci-cells in different phases of the cycle.

Image processing and statistics

To study the influence of CoCl₂ and DFO on the cell cycle, the fluorescent images were processed to count, in each field, the number of fluorescent cells. An example of the images we used is given on figure 1B. We used ImageJ (ImageJ 1.46a) and Matlab (Mathworks 2012a) to analyze these fluorescence data. The images are filtered to eliminate noise, and binarized to isolate the cells. We then create masks that we apply to the original images to extract the red and green fluorescences. If they are superior to the noise, they are taken into account to identify the cell phase. The non-fluorescent cells (M/G0/G1init) are manually counted. Thus, the percentage P of cells in each phase is obtained for each field of the cover-glass considered. To statistically estimate the mean value of P, we consider in this cover-glass 10 samples of more than 500 cells. In this way, the value of P and its standard deviation is obtained for each experimental conditions. We statistically compared these values of P by using Student tests. Four independent series of experiments were performed in order to test the reproducibility of the results.

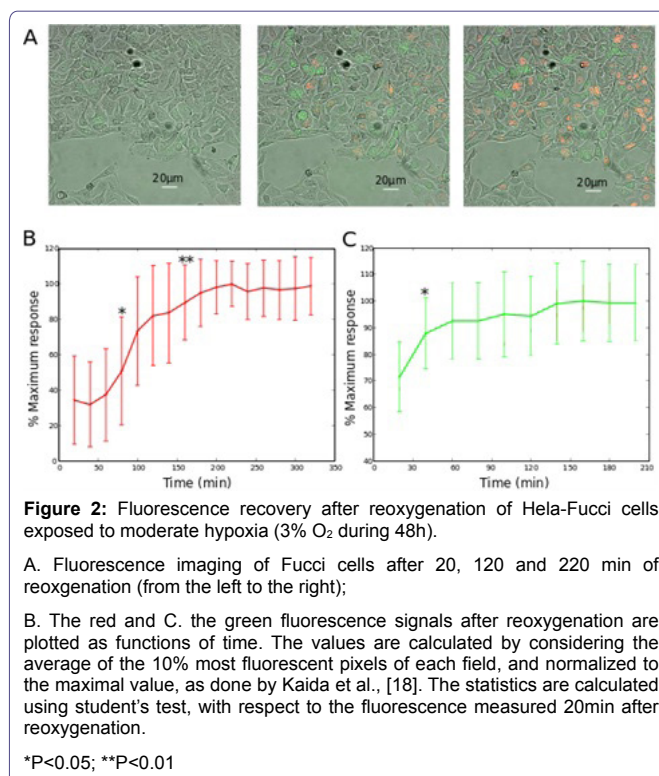
Results

Fluorescence extinction of HeLa-Fucci cells in hypoxic conditions

HeLa-Fucci cells are known to lose their fluorescence under hypoxia [19]. According to Kaida and Miura (2012) [20], this is due to the expression of proteins containing non-oxidized chromophores. We first submitted HeLa-Fucci cells to moderate hypoxia to verify if the extinction occurs in such smoother condition. First observations made after an exposure of 48h at 3% O₂ confirm the existence of a phenomenon of fluorescence extinction. The fluorescence is recovered after 3 hours in normoxia. Figure 2A, shows this effect of hypoxic loss and normoxic recovery of fluorescence in a representative field of cells on a cover-glass cultured at 3% O₂ and observed a long time in normoxic conditions. Following the same methods as Kaida et al., [19], we quantified this fluorescence recovery of Kusabira Orange 2 and monomeric Azami Green. After 48h at 3% O₂, the cells were reoxygenated and we followed the time evolution of the maximum fluorescence response for the two fluorescence channels. The results presented were obtained by sampling a cover-glass into forty microscopic fields, with more than fifty cells in each one. Images were taken every twenty minutes for about five hours. The maximum fluorescence was extracted along time in each of these fields, and the average fluorescence calculated. Figure 2B shows that the maximum red fluorescence increases for almost 2 hours. Figure 2C shows that the green fluorescence is less affected. Thus, even under moderate hypoxia, the artefact linked to the fluorescence extinction exists and makes difficult the use of HeLa-Fucci cells to study the cell cycle dynamics under real hypoxia. That is why it is necessary to test the relevance of the hypoxia-mimetic chemicals DFO and CoCl₂ to simulate the effects of a lack of oxygen on cell proliferation.

Estimation of DFO and CoCl₂ toxicity

In order to determine the range of concentrations to be used, we first investigated the toxicity of DFO and CoCl₂ after 48h of treatment for our cell line. For DFO, we found a significant increase of cell death for a concentration of 1mM, compared to a control cultured in the same conditions but without DFO. In the case of CoCl₂, this threshold concentration is 400 μM (data not shown). Both values are much higher than those reported for other cell lines. For example, the apoptotic ratio is already significant at 200 μM CoCl₂ for PC-2 cells



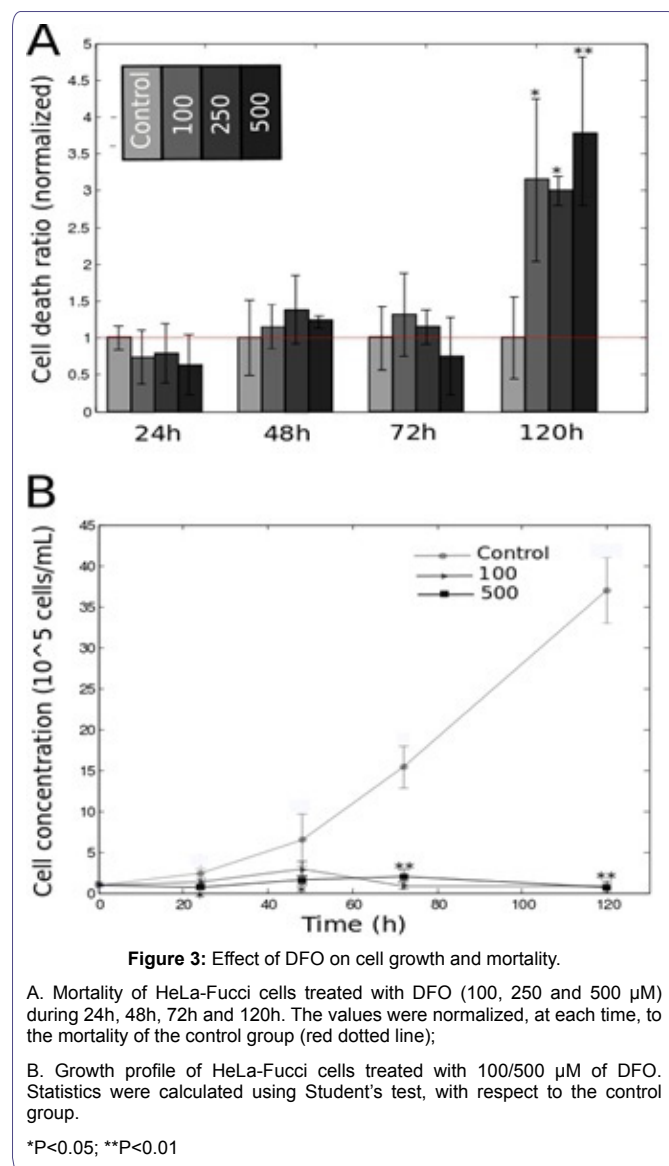
[25] and also for mouse embryonic stem cells where Lee et al., [26] have reported a mortality ratio of 40% after 48h at 150 mM CoCl₂. For DFO, Guo et al., [8] found an effect of a 48h exposure to DFO on cell death for a concentration of 100 μM. As a consequence, it appears that the toxicity of these molecules strongly depends on the cell line. In order to isolate the effects of DFO and CoCl₂ on the cell cycle from its influence in inducing cell death, we limited the use of these molecules to their non-toxic concentration range. In the rest of the study, we then used concentrations up to 500 μM for DFO, and up to 200 μM for CoCl₂.

DFO promotes cell death and inhibits cell growth

We first measured the mortality (or cell death ratio) for different concentrations of DFO, at 24h, 48h, 72h, and 120h. Figure 3A, shows the evolution of mortality after a treatment from 24 to 120 hours by 0, 100, 250 or 500 μM DFO. We observe that the influence of DFO on cell death is visible after a relatively important delay. Indeed, for the concentrations we used, DFO has no effect before 120h of treatment. Thus, HeLa-Fucci cells are relatively resistant to long-term toxicity of DFO, since Renton et al., [35] found a toxic effect at 10 μM DFO after 3 days in glioma cells. We then built the cell growth profile by evaluating the total cell concentration (live and dead cells) in the culture (Figure 3B). DFO inhibits cell growth, and this effect is not due to cell death. As a consequence, it may be due to its influence on the cell cycle dynamics.

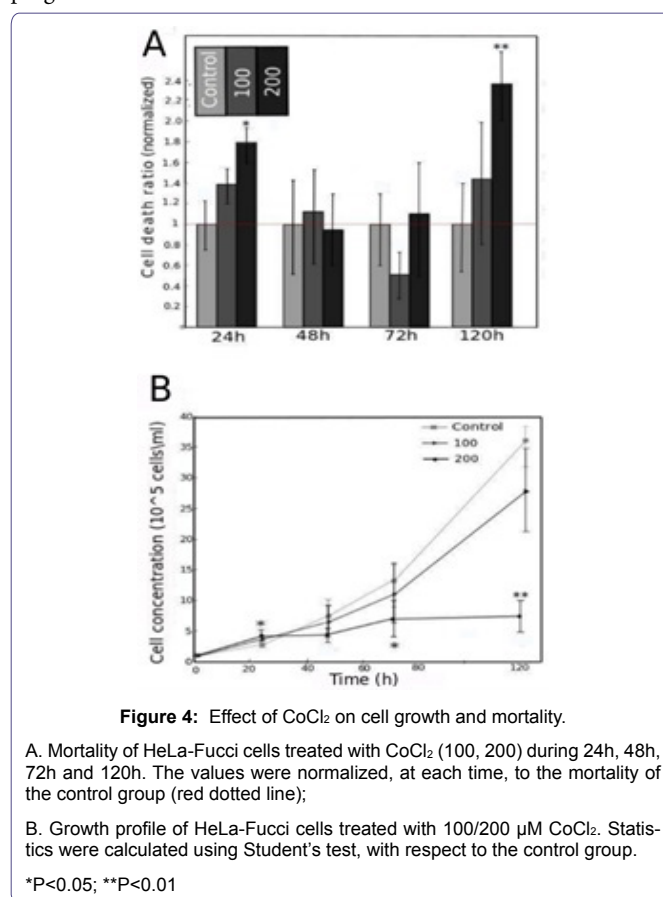
Dose and time dependency of CoCl₂ effect on cell death and growth

We did the same work with CoCl₂, for 0, 100 and 200 μM (Figure 4). The results obtained exhibit a more complex cellular response. We first observe three steps in the evolution of the cell death ratio. At 24h, CoCl₂ induces cell death (multiplied by 1.8 compared to control for the 200 μM group). After this first response of the cells to



the chemical agent, CoCl₂ has a zero (at 48h) or negative effect (at 72h, 100 μM group) on mortality. Then, at 120h, CoCl₂ induces cell death. The action of CoCl₂ is time and dose dependent, with a complex evolution during the treatment. At short and long time-scales, CoCl₂ promotes cell death. At a medium time-scale, it does not have any effects. The growth profile shows that at the beginning of the treatment (24h), the cells concentration in the CoCl₂-treated groups is more important than in the control group (increase of 50% for the 200 μM group compared to control). This observation is statistically significant (P<0.05). Therefore, cell growth is stimulated by CoCl₂. As mortality is more important at 24h in the CoCl₂-treated group than in the control group, this increase of cell concentration is certainly due to a stimulation of cell division. At the opposite, after 48h of treatment, an inhibition of cell growth is observed for the 200 μM group (decrease of 45% at 72h). This behavior must be due to an inhibition of cell division, up to 120h. After this time, the increase of the dead cells ratio may influence the population growth. The 100 μM group grows with the same kinetics as the control group. These results show that CoCl₂ and DFO have very different influences on cell death and cell growth. DFO rapidly inhibits cell proliferation, and

induces cell death after 120h. CoCl₂ acts in a more complex manner. It promotes cell death, and inhibits or promotes cell growth depending on dose and time of exposure. The comparison between mortality and population growth enables to estimate the division rate of the cell. For CoCl₂, at 24h, a reasonable hypothesis is that the proliferation rate is higher for the 200 μM group than for the control group, since the population growth is more rapid whereas the mortality is higher. As a consequence, our results with HeLa-Fucci cells suggest that the biphasic effect observed in population growth is most probably due to modifications of the cell cycle dynamics. In a similar way, the inhibition of cell growth in the DFO-treated groups is not due to an increase of mortality, but certainly to a blockage of cell cycle progression.



DFO promotes cell cycle arrest in G2 phase of HeLa-Fucci cells

By using fluorescent microscopy, we first imaged the progression of the cell cycle in control and DFO-treated groups. Figure 5, gives a representative example of the observed effects of DFO on the cell cycle. Compared to the control group, the cells treated during 24h with a 500 μM solution of DFO visibly show a more important proportion of green cells. This observation suggests that DFO tends to block the cell cycle during the G2 phase. In order to test and precise this hypothesis, we quantified the temporal evolution of the G2 phase proportion for populations treated with a large range of DFO concentrations, from 10 to 500 μM. Figure 6, presents the results. They were calculated using the statistical method described in the material and methods section. We first observe that DFO has an effect on the cell cycle for concentrations bigger than 10 μM. For concentrations from 25 to 500 μM, the proportion of cells in the G2 phase is above

80% after 72h. It means that nearly all the cells are blocked in the G2 phase. The kinetics of cell cycle arrest strictly depends in this case on DFO concentration. Thus, the DFO-mediated cell cycle arrest in the G2 phase appears to be a switch-like phenomenon. At low concentration, there is no effect. When the DFO level reaches a threshold, more than 80% of the cells are blocked after 72h. The kinetics of this blockage at the population scale depends on the DFO concentration.

CoCl₂ has a biphasic effect on HeLa-Fucci cells proliferation dynamics

We then applied the same protocol to characterize the influence of CoCl₂ on the cell cycle dynamics. By using the cell cycle phase definition described in the material and methods section, we could measure the ratio of non-cycling cells (G0/G1init cells). We performed this measurement for control, 100 μM and 200 μM groups, after 24h and 72h of treatment (Figure 7). At 24h, CoCl₂ decreases the ratio of G0/G1init cells (decrease of 35% for 100 μM and 30% for 200 μM compared to control). At 72h, the 100 μM group does not show any significant changes in G0/G1init ratio compared to the control group. The 200 μM group is characterized by a 150% increase of G0/G1init ratio compared to control. Interestingly, there is no significant change in the G2 +M and G0 +G1 cells percentage (data not shown). The reproducibility of these results was tested with four independent series

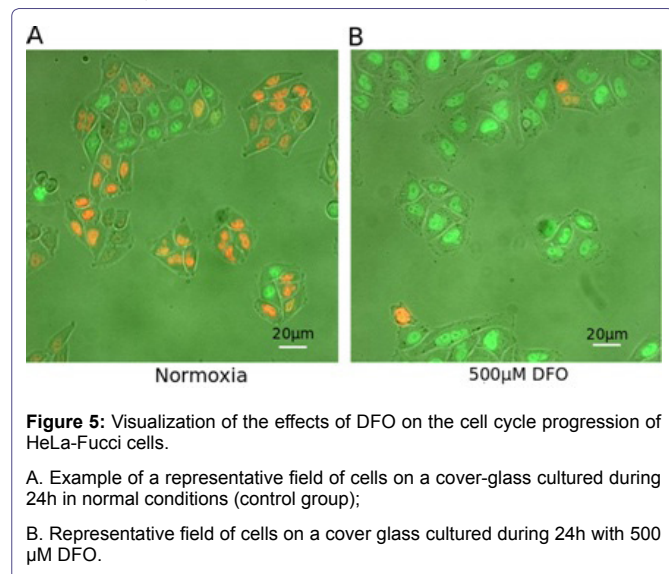


Figure 5: Visualization of the effects of DFO on the cell cycle progression of HeLa-Fucci cells.

A. Example of a representative field of cells on a cover-glass cultured during 24h in normal conditions (control group);

B. Representative field of cells on a cover glass cultured during 24h with 500 μM DFO.

of experiments. These observations thus suggest that CoCl₂ influences the transition between G0/G1init and G1 phase, that is to say the entry into the cycle. We conclude that the HiF-1α inducer CoCl₂ modulates the ability of the cells to begin their cycle. Interestingly, this influence of CoCl₂ is biphasic, and determined by time and dose. After 24h of treatment, CoCl₂ strongly promotes the entry into the cycle. At 72h, this effect vanishes for the 100 μM group, and is reversed for the 200 μM group. CoCl₂ becomes an inhibitor of the entry into the cell cycle.

Discussion

In this work, we tested for the first time, on HeLa-Fucci cells, the effects on cell death, cell growth and cell cycle of two widely used hypoxia-mimetic molecules (DFO and CoCl₂). Our principal result concerns the characterization of the cell cycle dynamics using fluorescent microscopy. We found that CoCl₂ has a biphasic effect on this cell line. It first promotes the progression into the G0/G1 phase,

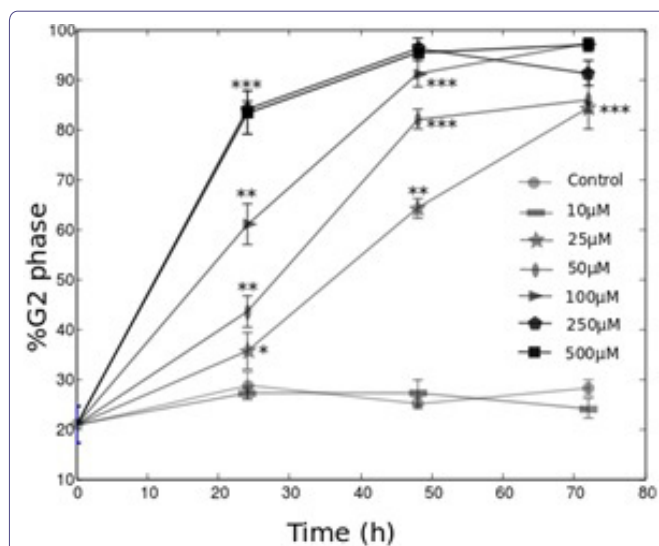


Figure 6: Time evolution of the percentage of cells in the G2 phase in cultures submitted to different levels of DFO.

The ratio (expressed in %) of HeLa-Fucci cells in the G2 phase is measured along time, for various concentrations of DFO (from gray to black : control, 10 μM, 25 μM, 50 μM, 100 μM, 250 μM, 500 μM). Statistics were calculated using Student's test, with respect to the control group.

*P<0.05; **P<0.001; ***P<0.0001

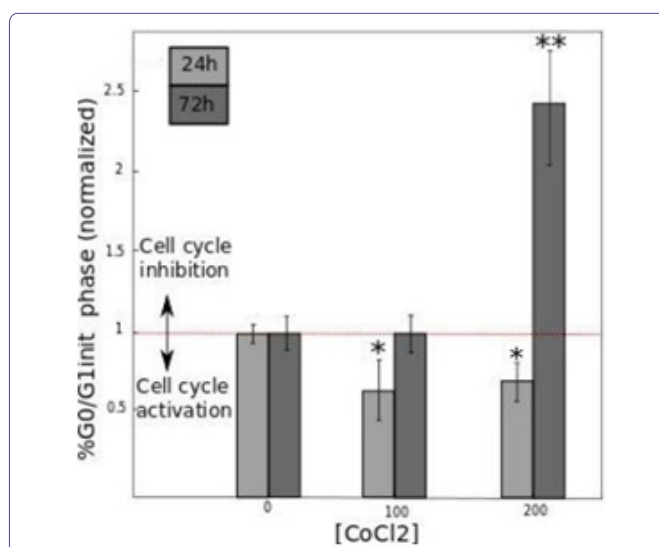


Figure 7: Effect of CoCl₂ on the entry into the cell cycle.

The ratio of HeLa-Fucci cells which have stopped cycling (G0/G1init cells) is measured after a 24h or 72h treatment with 100 or 200 μM CoCl₂, and normalized to the normoxic value (horizontal red dotted line). The statistics were calculated using student's test, with respect to the control group (without CoCl₂).

*P<0.001; **P<0.0005

and inhibits it in a second time. DFO was found to induce cell cycle arrest in the G2 phase, following a switch-like behavior. When its concentration reaches a threshold (10 μM), more than 80% of the cells stop in this phase with a kinetics depending on DFO concentration. This observation leads to various types of conclusions. First, it provides interesting information about the use of hypoxia-mimetic agents on Fucci cells. We notably found that the effects of the molecules used are different from the known cellular response of

hypoxia, which tends to promote cell cycle arrest in the G1 phase [9,37,38]. We note here that the use of HeLa-Fucci cells allowed us to distinguish the G0 from a G1init phase, which would not have been possible with other techniques such as flow cytometry. We could thus precisely quantify the effects of CoCl₂ on the entry into the cycle. From our work, it appears that DFO and CoCl₂ certainly have a large range of biological effects on HeLa-Fucci cells which hides the consequences of HiF-1 α induction. This conclusion shows strong obstacles to the use of HeLa-Fucci cells to study the effect of hypoxia on the cell cycle. However, since we have shown that the fluorescence recovers after about 2-3 hours in normoxia, this cell line can be a good tool to study the influence of reoxygenation on the cell cycle dynamics. The tools we developed in this study could be used towards this interesting perspective.

Second, the cellular response to iron-depletion has been intensely studied over these last years [22]. In this framework, the results we obtained with the HeLa-Fucci cell line are surprising. Whereas these two molecules were often shown to promote cell cycle arrest in the G1 or S phases, they act differently in the HeLa-Fucci cell line. The biphasic effect of CoCl₂ on cell growth was reported in the study by Dai et al., [25], but the authors did not explain this observation by precisely studying the cell cycle dynamics. As the Fucci cells allow us to follow the G0/G1 progression (non-colored to red cells), we could observe the biphasic effect of CoCl₂ on the entry into the cycle. Moreover, the G2 phase arrest in presence of DFO was rarely observed [22]. How can we explain the particular features of the response of HeLa-Fucci to iron-chelators DFO and CoCl₂? In their review, Yu et al., [22] note that one of the principal actor of the G1/S arrest in presence of these molecules is the p53 protein, which inhibits the cyclins D and E. Yet, HeLa cells are known to have low p53 activity [39-41]. This could explain the absence of a G1 phase arrest. This idea is confirmed by the fact that the cell lines exhibiting a G1 phase arrest in presence of DFO or CoCl₂ seem to present a wild-type p53 activity: hMSC [24], UCC-2 [29], T-Lymphocytes [32]. Interestingly, the study by Brodie et al., [31] quantified the proliferation of two cell lines in presence of DFO. The SKN-SH cell line (neuroblastoma) is very sensitive to the G1 phase arrest. It has a non-mutated p53 activity, as suggested by the results of Kim et al., [42]. On the contrary, the T98G cell line (glioblastoma) is not sensitive to the G1 phase arrest, and it presents a low p53 activity [43]. The low p53 activity of HeLa cells is also coherent with the high resistance to apoptosis we observed in this study. If p53 cannot explain the cell response to DFO and CoCl₂, which pathway could be involved?

The MAPK signaling cascade is strongly activated by iron-chelators [22]. More specifically, it was shown that DFO and CoCl₂ activate this pathway [30,44-46]. Besides, it is functional in the HeLa cell line [47,48]. The enzymes of the MAPK family, notably p38, ERK and MEK have numerous effects on the cell cycle. First, they are known to inhibit the G2/M transition, and to promote the G2 phase arrest of the cell cycle [49]. Second, it was shown that they have an effect on the G0/G1 progression. On the one hand, ERK1/2 can inhibit the progression into the G0/G1 phase by promoting the synthesis of Mirk/Dyrk1B [50]. On the second hand, it was recently shown that in HeLa cells, ERK1/2 promotes proliferation by activating the progression into the G1 phase [51]. Thus, ERK can have two opposite effects on cell proliferation. It provides a promising candidate (or mechanism?) to explain the biphasic response to CoCl₂ we observed with HeLa-Fucci cells.

Interestingly, a biphasic effect related to MAPK activation by Cd and Hg was observed by Hao et al., [52]. As a consequence, our hypothesis that the response of HeLa-Fucci cells to CoCl₂ treatment is due to the activation of the MAPK pathway may be relevant. Following this view, in presence of CoCl₂, proteins activating cell proliferation are primarily synthesized. The work of Bai et al., [51] suggests that the p-c-fos protein could be involved in this step. Then, Mirk/Dyrk1B gene is expressed, and the progression into the G0/G1 phase is slowed down. As our experiments show that the biphasic time-response to CoCl₂ is coupled to a biphasic dose-response, we can suggest that the differential activation of the Mirk and p-c-fos pathways could also depend on the concentration of the chemical. However, in this framework, it remains difficult to understand why DFO and CoCl₂ have different actions on the cell cycle dynamics. It may depend on the type of enzymes activated by each of these agents. DFO would activate the MAPK-mediated G2 phase arrest and CoCl₂ the biphasic action of MAPK on the G0/G1 progression. The complexity of the MAPK pathway and the huge number of its targets do not allow us to propose a more precise hypothesis. In all cases, the idea of a predominance of the MAPK pathway, because of the inactivity of p53, is an interesting hypothesis. It could be tested with molecular biology protocols. There would be many approaches to test. That is why we chose to limit our work to a first investigation at the cellular scale. For instance, it would be interesting to observe the effects of chemical inhibitions of the MAPK signaling cascade, as made in previous studies [49,51]. If our hypothesis is verified, HeLa-Fucci cells would be a good tool to precisely study the poorly known impact of iron-chelators agents on the MAPK pathway.

Acknowledgment

We acknowledge RIKEN BioResource Center for providing and allowing us to use the FUCCI cells (Biological resource RCB 2812). We also thank Dr Didier Wion for helpful discussion and for providing hypoxia facilities

References

1. Sakaue-Sawano A, Kurokawa H, Morimura T, Hanyu A, Hama H, et al. (2008) Visualizing spatiotemporal dynamics of multicellular cell-cycle progression. *Cell* 132: 487-498.
2. Sugiyama M, Sakaue-Sawano A, Iimura T, Fukami K, Kitaguchi T, et al. (2009) Illuminating cell-cycle progression in the developing zebrafish embryo. *Proc Natl Acad Sci USA* 106: 20812-20817.
3. Zielke N, Korzelius J, van Straaten M, Bender K, Schuhknecht GF, et al. (2014) Fly-FUCCI: A versatile tool for studying cell proliferation in complex tissues. *Cell Rep* 7: 588-598.
4. Harris AL (2002) Hypoxia--a key regulatory factor in tumour growth. *Nat Rev Cancer* 2: 38-47.
5. Lesart AC, van der Sanden B, Hamard L, Estève F, Stéphanou A (2012) On the importance of the submicrovascular network in a computational model of tumour growth. *Microvasc Res* 84: 188-204.
6. Hernandez-Luna MA, Rocha-Zavaleta L, Vega MI, Huerta-Yepez S (2013) Hypoxia inducible factor-1 α induces chemoresistance phenotype in non-Hodgkin lymphoma cell line via up-regulation of Bcl-xL. *Leuk Lymphoma* 54: 1048-1055.
7. Kunz M, Ibrahim SM (2003) Molecular responses to hypoxia in tumor cells. *Mol Cancer* 2: 23.
8. Guo M, Song LP, Jiang Y, Liu W, Yu Y, et al. (2006) Hypoxia-mimetic agents desferrioxamine and cobalt chloride induce leukemic cell apoptosis through different hypoxia-inducible factor-1 α independent mechanisms. *Apoptosis* 11: 67-77.

9. Gardner LB, Li Q, Park MS, Flanagan WM, Semenza GL, et al. (2001) Hypoxia inhibits G1/S transition through regulation of p27 expression. *J Biol Chem* 276: 7919-7926.
10. Gwak GY, Yoon JH, Kim KM, Lee HS, Chung JW, et al. (2005) Hypoxia stimulates proliferation of human hepatoma cells through the induction of hexokinase II expression. *J Hepatol* 42: 358-364.
11. Michiels C, De Leener F, Arnould T, Dieu M, Remacle J (1994) Hypoxia stimulates human endothelial cells to release smooth muscle cell mitogens: role of prostaglandins and bFGF. *Exp Cell Res* 213: 43-54.
12. Sahai A, Mei C, Pattison TA, Tannen RL (1997) Chronic hypoxia induces proliferation of cultured mesangial cells: role of calcium and protein kinase C. *Am J Physiol* 273: 954-960.
13. Wohrley JD, Frid MG, Moiseeva EP, Orton EC, Belknap JK, et al. (1995) Hypoxia selectively induces proliferation in a specific subpopulation of smooth muscle cells in the bovine neonatal pulmonary arterial media. *J Clin Invest* 96: 273-281.
14. Sermeus A, Michiels C (2011) Reciprocal influence of the p53 and the hypoxic pathways. *Cell Death Dis* 2: 164.
15. Semenza GL (2007) Hypoxia-Inducible Factor 1 (HIF-1) pathway. *Sci STKE* 2007: cm8.
16. Ke Q, Costa M (2006) Hypoxia-Inducible Factor-1 (HIF-1). *Mol Pharmacol* 70: 1469-1480.
17. Zhong H, De Marzo AM, Laughner E, Lim M, Hilton DA, et al. (1999) Overexpression of hypoxia-inducible factor 1alpha in common human cancers and their metastases. *Cancer Res* 59: 5830-5835.
18. Banks RE, Tirukonda P, Taylor C, Hornigold N, Astuti D, et al. (2006) Genetic and epigenetic analysis of Von Hippel-Lindau (VHL) gene alterations and relationship with clinical variables in sporadic renal cancer. *Cancer Res* 66: 2000-2011.
19. Kaida A, Miura M (2012) Differential dependence on oxygen tension during the maturation process between monomeric Kusabira Orange 2 and monomeric Azami Green expressed in HeLa cells. *Biochem Biophys Res Commun* 421: 855-859.
20. Kaida A, Miura M (2012) Visualizing the effect of hypoxia on fluorescence kinetics in living HeLa cells using the Fluorescent ubiquitination-based cell cycle indicator (Fucci). *Exp Cell Res* 318: 288-297.
21. Potuckova E, Jansova H, Machacek M, Vavrova A, Haskova P, et al. (2014) Quantitative analysis of the anti-proliferative activity of combinations of selected iron-chelating agents and clinically used anti-neoplastic drugs. *PLoS One* 9: 88754.
22. Yu Y, Kovacevic Z, Richardson DR (2007) Tuning cell cycle regulation with an iron key. *Cell Cycle* 6: 1982-1994.
23. Xiao H, Gu Z, Wang G, Zhao T (2013) The possible mechanisms underlying the impairment of HIF-1 α pathway signaling in hyperglycemia and the beneficial effects of certain therapies. *Int J Med Sci* 10: 1412-1421.
24. Zeng HL, Zhong Q, Qin YL, Bu QQ, Han XA, et al. (2011) Hypoxia-mimetic agents inhibit proliferation and alter the morphology of human umbilical cord-derived mesenchymal stem cells. *BMC Cell Biol* 12: 32.
25. Dai ZJ, Gao J, Ma XB, Yan K, Liu XX, et al. (2012) Up-regulation of hypoxia inducible factor-1 α by cobalt chloride correlates with proliferation and apoptosis in PC-2 cells. *J Exp Clin Cancer Res* 31: 28.
26. Lee JH, Choi SH, Baek MW, Kim MH, Kim HJ, et al. (2013) CoCl₂ induces apoptosis through the mitochondria- and death receptor-mediated pathway in the mouse embryonic stem cells. *Mol Cell Biochem* 379: 133-140.
27. Ardyanto TD, Osaki M, Tokuyasu N, Nagahama Y, Ito H (2006) CoCl₂-induced HIF-1alpha expression correlates with proliferation and apoptosis in MKN-1 cells: a possible role for the PI3K/Akt pathway. *Int J Oncol* 29: 549-555.
28. Piret JP, Mottet D, Raes M, Michiels C (2002) CoCl₂, a chemical inducer of hypoxia-inducible factor-1, and hypoxia reduce apoptotic cell death in hepatoma cell line HepG2. *Ann N Y Acad Sci* 973: 443-447.
29. Bae S, Jeong HJ, Cha HJ, Kim K, Choi YM, et al. (2012) The hypoxia-mimetic agent cobalt chloride induces cell cycle arrest and alters gene expression in U266 multiple myeloma cells. *Int J Mol Med* 30: 1180-1186.
30. Triantafyllou A, Liakos P, Tsakalof A, Georgatsou E, Simos G, et al. (2006) Cobalt induces Hypoxia-Inducible Factor-1alpha (HIF-1alpha) in HeLa cells by an iron-independent, but ROS-, PI-3K- and MAPK-dependent mechanism. *Free Radic Res* 40: 847-856.
31. Brodie C, Siriwardana G, Lucas J, Schleicher R, Terada N, et al. (1993) Neuroblastoma sensitivity to growth inhibition by deferrioxamine: evidence for a block in G1 phase of the cell cycle. *Cancer Res* 53: 3968-3975.
32. Lucas JJ, Szepesi A, Domenico J, Takase K, Tordai A, et al. (1995) Effects of iron-depletion on cell cycle progression in normal human T lymphocytes: selective inhibition of the appearance of the cyclin A-associated component of the p33cdk2 kinase. *Blood* 86: 2268-2280.
33. Metzendorf C, Lind MI (2010) The role of iron in the proliferation of *Drosophila* l(2) mbn cells. *Biochem Biophys Res Commun* 400: 442-446.
34. Siriwardana G, Seligman PA (2013) Two cell cycle blocks caused by iron chelation of neuroblastoma cells: separating cell cycle events associated with each block. *Physiol Rep* 1: 00176.
35. Renton FJ, Jeitner TM (1996) Cell cycle-dependent inhibition of the proliferation of human neural tumor cell lines by iron chelators. *Biochem Pharmacol* 51: 1553-1561.
36. Nagano T, Hashimoto T, Nakashima A, Hisanaga S, Kikkawa U, et al. (2013) Cyclin I is involved in the regulation of cell cycle progression. *Cell Cycle* 12: 2617-2624.
37. Box AH, Demetrick DJ (2004) Cell cycle kinase inhibitor expression and hypoxia-induced cell cycle arrest in human cancer cell lines. *Carcinogenesis* 25: 2325-2335.
38. Goda N, Dozier SJ, Johnson RS (2003) HIF-1 in cell cycle regulation, apoptosis, and tumor progression. *Antioxid Redox Signal* 5: 467-473.
39. Koivusalo R, Krausz E, Helenius H, Hietanen S (2005) Chemotherapy compounds in cervical cancer cells primed by reconstitution of p53 function after short interfering RNA-mediated degradation of human papillomavirus 18 E6 mRNA: opposite effect of siRNA in combination with different drugs. *Mol Pharmacol* 68: 372-382.
40. May E, Jenkins JR, May P (1991) Endogenous HeLa p53 proteins are easily detected in HeLa cells transfected with mouse deletion mutant p53 gene. *Oncogene* 6: 1363-1365.
41. Minagawa Y, Kigawa J, Itamochi H, Kanamori Y, Shimada M, et al. (1999) Cisplatin-resistant HeLa cells are resistant to apoptosis via p53-dependent and -independent pathways. *Jpn J Cancer Res* 90: 1373-1379.
42. Kim SS, Chae HS, Bach JH, Lee MW, Kim KY, et al. (2002) P53 mediates ceramide-induced apoptosis in SKN-SH cells. *Oncogene* 21: 2020-2028.
43. Park CM, Park MJ, Kwak HJ, Moon SI, Yoo DH, et al. (2006) Induction of p53-mediated apoptosis and recovery of chemosensitivity through p53 transduction in human glioblastoma cells by cisplatin. *Int J Oncol* 28: 119-125.
44. Gaitanaki C, Kalpachidou T, Aggeli IK, Papazafiri P, Beis I (2007) CoCl₂ induces protective events via the p38-MAPK signalling pathway and ANP in the perfused amphibian heart. *J Exp Biol* 210: 2267-2277.
45. Lee SK, Jang HJ, Lee HJ, Lee J, Jeon BH, et al. (2006) p38 and ERK MAP kinase mediates iron chelator-induced apoptosis and -suppressed differentiation of immortalized and malignant human oral keratinocytes. *Life Sci* 79: 1419-1427.
46. Markel TA, Crisostomo PR, Wang M, Herring CM, Lahm T, et al. (2007) Iron chelation acutely stimulates fetal human intestinal cell production of IL-6 and VEGF while decreasing HGF: the roles of p38, ERK, and JNK MAPK signaling. *Am J Physiol Gastrointest Liver Physiol* 292: 958-963.

47. An WW, Gong XF, Wang MW, Tashiro S, Onodera S, et al. (2004) Norcantharidin induces apoptosis in HeLa cells through caspase, MAPK, and mitochondrial pathways. *Acta Pharmacol Sin* 25: 1502-1508.
48. Zhong W, Zhu H, Sheng F, Tian Y, Zhou J, et al. (2014) Activation of the mapk11/12/13/14 (p38 mapk) pathway regulates the transcription of autophagy genes in response to oxidative stress induced by a novel copper complex in HeLa cells. *Autophagy* 10:1285-1300.
49. Astuti P, Pike T, Widberg C, Payne E, Harding A, et al. (2009) MAPK pathway activation delays G2/M progression by destabilizing Cdc25B. *J Biol Chem* 284: 33781-33788.
50. Gao J, Zhao Y, Lv Y, Chen Y, Wei B, et al. (2013) Mirk/Dyrk1B mediates G0/G1 to S phase cell cycle progression and cell survival involving MAPK/ERK signaling in human cancer cells. *Cancer Cell Int* 13: 2.
51. Bai L, Mao R, Wang J, Ding L, Jiang S, et al. (2015) ERK1/2 promoted proliferation and inhibited apoptosis of human cervical cancer cells and regulated the expression of c-Fos and c-Jun proteins. *Med Oncol* 32: 57.
52. Hao C, Hao W, Wei X, Xing L, Jiang J, et al. (2009) The role of MAPK in the biphasic dose-response phenomenon induced by cadmium and mercury in HEK293 cells. *Toxicol In Vitro* 23: 660-666.